THESIS FOR THE DEGREE OF LICENTIATE OF ENGINEERING

Characterization of elastic moduli of single fibres

SHANGHONG DUAN

Department of Industrial and Materials Science

CHALMERS UNIVERSITY OF TECHNOLOGY

Gothenburg, Sweden 2020

Characterization of elastic moduli of single fibres
SHANGHONG DUAN

© SHANGHONG DUAN, 2020.

Technical report no IMS-2020-12
Department of Industrial and Materials Science
Chalmers University of Technology
SE-412 96 Gothenburg
Sweden
Telephone + 46 (0)31-772 1000

Cover:
Representative picture of licentiate thesis

Chalmers Reproservice
Gothenburg, Sweden 2020

Characterization of elastic moduli of single fibres
Thesis for the degree of Licentiate of Engineering
SHANGHONG DUAN
Department of Industrial and Materials Science
Division of Material and Computational Mechanics
Chalmers University of Technology

Abstract

The carbon fibre is one of most promising materials for high-performance composites since it is lightweight and strong. It has been widely used to build carbon fibre reinforced polymer (CFRP) composites. The carbon fibre dramatically reinforces the composite in the fibre direction. However, carbon fibre does not significantly reinforce the composite transverse to the fibres. The reason is in addition to the fibre geometry, that the mechanical properties of carbon fibre are anisotropic. Even though the strong anisotropy is well known, to date only the properties in axial direction have been accurately measured. Measurements in other directions, like the transverse direction, are challenging because the diameter of carbon fibre is only 5 to 7 μm. Knowledge of the mechanical properties of carbon fibre is important, especially for micro-mechanical models to predict damage formation in CFRP. The small dimension of carbon fibre implies that only a limited set of instruments can be used to perform mechanical tests on it, such as nanoindentation and atomic force microscopy (AFM). Moreover, the high anisotropy of carbon fibre needs a special analysis method.

In this thesis, we first study a fabrication routine for preparation of flat surfaces on carbon fibres using a focussed ion beam technique. A necessary and effective cleaning process to remove damaged surface from fabrication process is presented. We then perform indentation tests using both nanoindentation and AFM in two different directions. During the tests, a hysteresis behaviour of carbon fibre was observed and its influence on indentation moduli is discussed. Finally, we successfully determine both transverse and shear moduli of three different carbon fibres.

Keyword: Carbon fibre, Transverse modulus, Shear modulus, AFM, Nanoindentation

Preface

The present work was performed from December 2017 to November 2020 at the Division of Material and Computational Mechanics, Department of Industrial and Materials science, Chalmers University of Technology. The project is funded by the European Union, Clean Sky Joint Undertaking 2, Horizon 2020 under Grant Agreement Number 738085 and USAF, contract FA9550-17-1-0338.

Acknowledgements

First, I would like to thank my main supervisor Prof. Leif Asp for his great guidance and support in last three years. His wide knowledge and network made this work possible. I am grateful for the extremely nice working and study environment at Chalmers. He always supported me to do research that I am interested in. It is a great honour to be a student of Leif.

I would also like to thank my co-supervisor Prof. Fang Liu. Fang is patient and always available for discussion. Her extensive knowledge at electron microscopy is one of the key factors of this work. I learned a lot from her. I would also thank all my friends and colleges at Chalmers, especially my teammates David Carlstedt and Johanna Xu. I really enjoy the nice teamwork and all the interesting discussions. They make the work much more fun.

Finally, I would like to thank my girlfriend Yuyin Jin. Her accompany and support are the most important driving force to me. I couldn’t accomplish this work without her.

Gothenburg 2020

Shanghong Duan

Thesis

This thesis consists of an extended summary and the following appended papers:

Paper A: Liu F, **Duan S** and Asp LE. "Specimen preparation for transverse modulus measurement of carbon Fibres using focused ion beam". *Proceedings of 22nd International Conference of Composite Materials (ICCM22)*, Melbourne, AUS, 2019.

Paper B: **Duan S**, Liu F, Pettersson T, Creighton C, Asp LE. "Transverse modulus measurement of carbon fibre by Atomic force microscope and nanoindentation". *Proceedings of 22nd International Conference of Composite Materials (ICCM22)*, Melbourne, AUS, 2019.

Paper C: **Duan S**, Liu F, Pettersson T, Creighton C, Asp LE. "Determination of transverse and shear moduli of single carbon fibres". *Carbon*. Vol. 158C, 2020, pp. 772-782.

Table of Contents

Part I

Extended Summary

1 Introduction

Carbon fibre is a promising lightweight material, which has been used widely in carbon fibre reinforced polymer (CFRP). Comparing with traditional materials, e.g. steel, carbon fibre has around 10 times higher specific stiffness and strength in the fibre direction [1], great corrosion resistance and high temperature performance. However, carbon fibres are also highly anisotropic. For example, the Young's modulus in the radial (i.e. transverse) direction is typically considered to be around 10 % of that in the fibre's longitudinal direction. Anisotropy occurs because the graphene planes in the carbon fibre are mainly aligned in the fibre direction. In the graphene plane, the carbon atoms are bonded by strong covalent bonds. Between the graphene layers, weak van der Waals bonds act. Accurate values for all moduli of carbon fibre is of great importance for all micromechanics models of CFRP [2, 3].

Even though the high anisotropy of carbon fibre is well-known, the exact mechanical properties of carbon fibre in all directions are not well studied. There are two main reasons for this. Firstly, the small diameter of the carbon fibre (~5 μm) makes sample preparation and mechanical tests very challenging. Secondly, the high anisotropy of carbon fibre also increases the difficulty of data analysis. There are few experimental works published to date which measure the transverse Young's modulus of carbon fibre using single fibre compression, ultrasonic scattering and nanoindentation tests [4-9]. The specimens are either raw carbon fibre or mechanically polished carbon fibre. Moreover, the high anisotropy was not well considered in the data analysis. Only Csanádi et. al. implemented a simplified orthotropic contact model to assess their data [9].

In this thesis, we study both experimental and analysis methods to determine transverse and shear moduli of carbon fibre. To increase the accuracy of the results, our specimens were fabricated using focused ion beam (FIB), which is normally used to fabricate transmission electron microscopy (TEM) specimen (100 nm thick foil). Two different instruments, atomic force microscopy (AFM) and nanoindentation, were employed to perform indentation tests on single carbon fibres. The difference between the results indicated a hysteresis indentation behaviour of carbon fibre. The hysteresis behaviour of carbon fibres has not been considered in any previous work. Furthermore, we modified the analysis method of AFM to obtain more accurate results when stiff carbon fibre was tested. Employing an orthotropic contact model [10], the transverse and shear moduli were calculated from the recorded indentation moduli.

2 Indentation tests

To perform mechanical tests on a single carbon fibre, limited methods are available, such as micro-compression test, nanoindentation test and ultrasonic scattering [4-9]. Among them, nanoindentation is the only one that generates multi-axial stress state in a specimen. Compression occurs in all directions and shear deformation also occurs during indentation. Therefore, the measured modulus cannot directly represent the modulus in the indentation direction. However, it also means the indentation modulus contains other information, such as shear modulus. With a correct model and combining indentation tests in different directions, all mechanical properties can be determined. Two indentation methods were used in this thesis: nanoindentation and atomic force microscopy (AFM).

2.1 Nanoindentation and its analysis model

Nanoindentation tests are conducted in Brucker's Hysitron TI 980 TriboIndenter. The nanoindentation employed a diamond Berkovich indenter (Fig. 1(a)). During the indentation test, the diamond indenter is pushed into the specimen body and both the force and indentation depth are recorded through a piezoelectric element. The approximate indentation depth in this work is around 100 nm. 3D morphology of the indenter tip is reconstructed using scanning probe microscopy (SPM). A polycarbonate (PC) reference material is used.

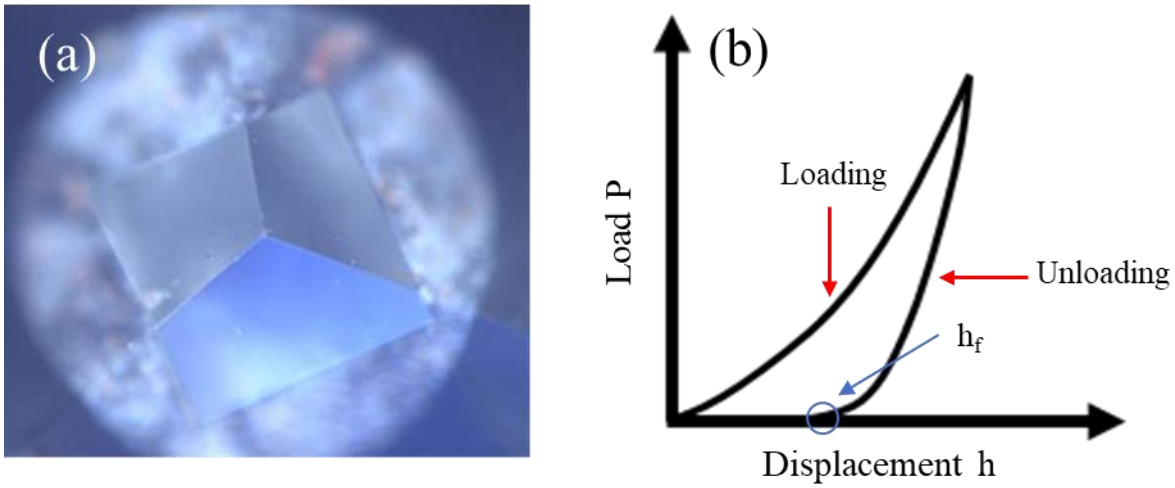

Figure 1. a) Optical microscopy photo of the Berkovich indenter. b) Typic indentation force-displacement curve.

The recorded Force-Displacement curve is analysed using the Pharr-Oliver contact model [11]. The unloading curve is fully elastic and assumed to be a power-law function,

$$P = \alpha\left(h - h_f\right)^m \tag{1}$$

where α is the force, h is the indentation depth, h_f is the permanent indentation depth (Fig. 1(b)), α and m are fitting parameters. The indentation modulus E^* can be calculated from the slop of the initial unloading curve S and contact area A_c,

$$E^* = \frac{S\sqrt{\pi}}{2\beta\sqrt{A_c}} \tag{2}$$

where β is the geometry factor. A_c can be obtained from the reconstructed 3D indenter tip from SPM. For an isotropic material, the indentation modulus E^* can be easily transformed to Young's modulus by

$$\frac{1}{E^*} = \frac{1-v_i^2}{E_i} - \frac{1-v^2}{E} \tag{3}$$

where v_i and v are the Poisson's ratios and E_i and E are the Young's moduli of indenter material and specimen, respectively. Note that carbon fibre is highly anisotropic. An orthotropic contact model is needed, as discussed in **Section 5**.

2.2 Atomic force microscopy and its analysis model

AFM is using a scanning probe microscopy technique. A schematic diagram of AFM is shown in Fig. 2. In this thesis, a MultiMode III with Picoforce extension (Veeco Instrument, Santa Barbara, CA, USA) was employed. A diamond probe with tip radius around 30 nm was purchased from Bruker™ company. Over 30 tests were performed on each specimen.

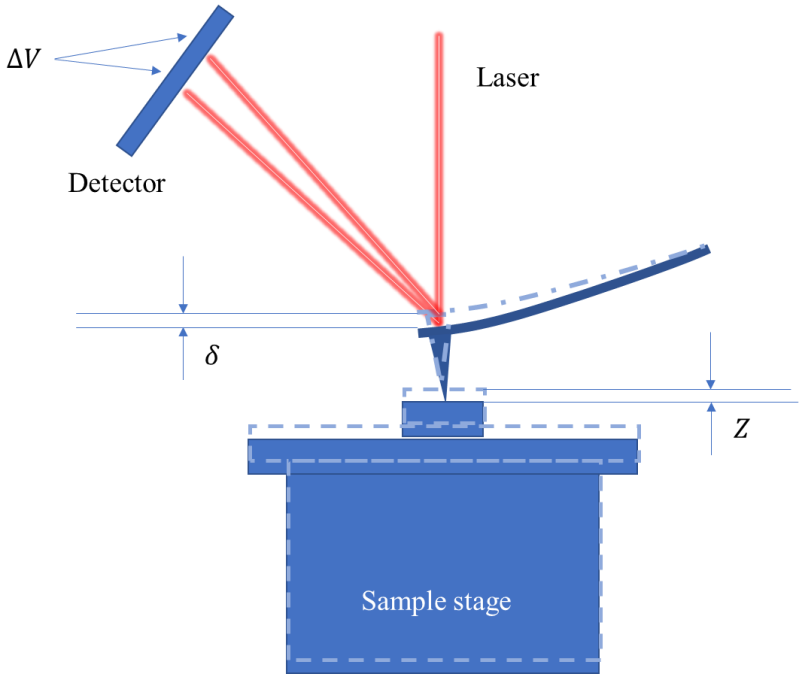

Figure 2. Schematic diagram of atomic force microscopy.

The indentation was performed in force mode. The sample stage moves up vertically under a control of a piezoelectric element. The displacement of the sample stage, Z, is recorded. After the specimen contacts with the probe. The probe cantilever starts to bend during following indentation. The bending of probe cantilever would cause a movement of the laser reflection spot on the detector screen, where a deflection voltage, ΔV, can be recorded. With assumption that the cantilever behaves as an ideal spring under small bending deformation, the indentation force F and displacement D can be calculated as

$$D = Z - \delta = Z - \Delta V \times \varepsilon \tag{4}$$

$$F = k \times \delta = k \times \Delta V \times \varepsilon \tag{5}$$

where k is the spring constant of the probe cantilever, δ is the deflection of the cantilever and ε is the detector sensitivity. The spring constant k varies between different probes and the detector sensitivity ε is sensitive to the installation of the probe. These two values must be calibrated by reference materials. For different direction indentation tests, different reference material was selected: a highly oriented pyrolytic graphite (HOPG) thin film (Young's modulus 18 GPa) was used for indentation in fibre transverse direction and fused silica (Young's modulus 72.9 GPa) was used for indentation in the fibre axial direction, respectively.

The indentation depth is controlled to be less than 10 nm, since our analysis method is based on an Hertzian contact model [12], which describes a pure elastic indentation of a sphere into a half surface. The force is a function of indentation depth as

$$F = \frac{4}{3} E^* \sqrt{R D^3} \tag{6}$$

where the R is the tip radius. However, the detector sensitivity is difficult to calibrate when a stiff specimen is tested. The traditional method is to perform indentation test on a sapphire reference material and assume the indentation depth to be zero. Sapphire is a relatively stiff material with a Young's modulus of 345 GPa. For soft materials, such a method is convenient and accurate. However, carbon fibre is also a stiff material (ranging from 230 GPa to 1000 GPa in the axial direction). For such stiff materials the assumption of zero indentation depth on sapphire cannot be applied. To eliminate the calibration error, we modified the analysis method in **Paper C**.

The miscalibration of detector sensitivity, $\Delta\varepsilon$, should generate the same displacement error, ΔD, for a give force load (ΔV is predefined) according to Eq. 4 and 5 That means even the displacement cannot be obtained correctly, the difference between specimen and reference material is still correct. Combining the Hertzian contact model,

$$D = F^{\frac{2}{3}} \left(\frac{4\sqrt{R}}{3} E^* \right)^{-\frac{2}{3}} = A {E^*}^{-\frac{2}{3}} \tag{7}$$

where A represents a constant when constant force is used. For each test, we employed two reference materials,

$$D_{specimen} = {D_{specimen}}' + \Delta D \tag{8}$$

$$D_{reference1} = {D_{reference1}}' + \Delta D \tag{9}$$

$$D_{reference2} = {D_{reference2}}' + \Delta D \tag{10}$$

where D' is the displacement obtained from experiment and ΔD is the unknown deviation from the true displacement due to the unknown calibration error. Subtracting Eq. 10 from Eq. 8 and 9,

$$\frac{D_{specimen} - D_{reference2}}{D_{reference1} - D_{reference2}} = \frac{{D_{specimen}}' - {D_{reference2}}'}{{D_{reference1}}' - {D_{reference2}}'} \tag{11}$$

Combining with Eq. 7,

$$\frac{{D_{specimen}}' - {D_{reference2}}'}{{D_{reference1}}' - {D_{reference2}}'} = \frac{{E^*_{specimen}}^{-\frac{2}{3}} - {E^*_{reference2}}^{-\frac{2}{3}}}{{E^*_{reference1}}^{-\frac{2}{3}} - {E^*_{reference2}}^{-\frac{2}{3}}} \tag{12}$$

Note that the left side of Eq. 12 can be obtained from experiment and $E^*_{reference1}$, $E^*_{referenc2}$ are known values of reference materials. The indentation modulus $E^*_{specimen}$ can be calculated without the need to accurately determine the calibration error.

3 Specimen preparation methods

To perform nanoindentation and AFM indentation tests on a single carbon fibre, a flat surface is needed. Considering the indentation depth of the AFM indentation test is limited to 10 nm, the flat surface needs an extremely low roughness. The minimum paste size for mechanical polishing is normally 1 μm. This is much larger than the size of AFM probe tip. Therefore, a more advanced technique, focused ion beam (FIB), is chosen to fabricate flat surfaces on carbon fibres. The fabrication was processed in Versa3D LoVac Duabeam electron scanning microscopy (SEM).

3.1 Surface fabrication

Two different type of surfaces were fabricated in this thesis: longitudinal and transverse cross-sections. Single fibres were adhesively bonded on a silicon wafer using silver glue. The fabricated section was additionally fixed by Pt deposition in the FIB-SEM. The Pt coating around the carbon fibre also helped to reduce surface damage in the following milling process. The carbon fibre was milled by high energy Ga^+ ions. The heavy Ga^+

ions were accelerated under high voltage (30 kV) towards and hit the carbon fibre. As a result carbon atoms were knocked out. In order to increase the surface quality, the milling process was divided into several steps. The current of the ion beam was reduced step by step (3 to 1 to 0.5 nA). The procedures of fabrication of longitudinal cross-section is shown in Fig. 3.

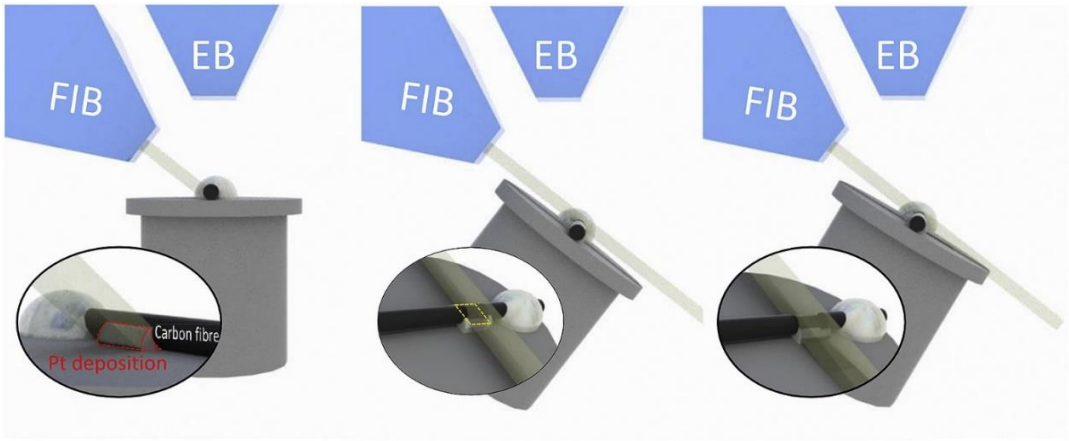

Figure 3. Fabrication process of longitudinal cross-section of carbon fibre (**Paper C**).

The fabrication of the transverse cross-section was similar. However, it involved more steps to adjust the geometry and place the short carbon fibre section standing on the substrate (Fig. 4).

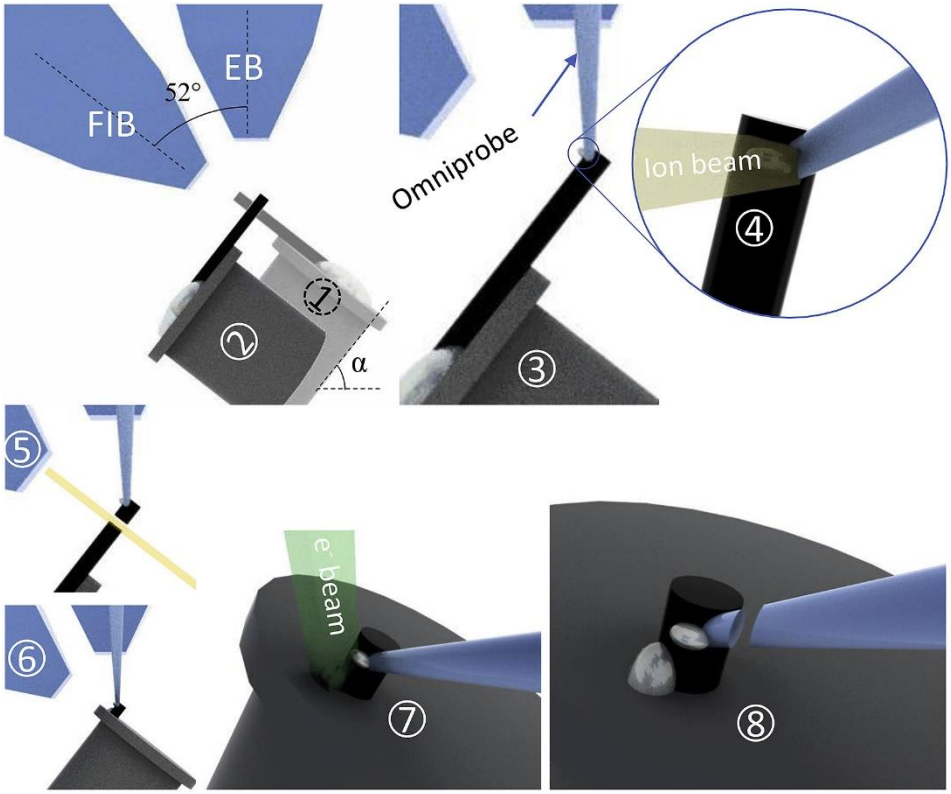

Figure 4. Fabrication process of transverse cross-section of carbon fibre (**Paper C**). Step 1 and 2: Positioning of carbon fibre. Step 3, 4, 5: Cutting of a short carbon fibre section. Step 6, 7, 8: move the short carbon fibre section to substrate.

3.2 Surface cleaning process

After FIB milling, a very flat surface is obtained. Even though it looks almost perfect, a very thin damaged layer on the top surface is expected. It is caused by the hitting and implant of Ga^+ ions. This damaged layer is amorphous and therefore expected to be a soft layer. The exact damage thickness is unknown. In silicon, such a damage layer can extend to tens of nanometres [13,14]. Considering that the indentation depth of AFM is around 10 nm, the damaged amorphous layer can significantly influence the results. To clean the surface, the most effective method is milling at low angle and using low energy ions. In silicon, 30 keV Ga^+ ions cause a 21 nm thick damaged layer. After re-milling using 5 keV Ga^+ ions, the damaged layer is reduced to 2 nm [15]. In this thesis, we reduced the energy of Ga^+ ions to 5 keV and tilted the milled surface by 7°.

To verify the cleaning process, we did a comparison test in **Paper B**. We prepared specimens with and without cleaning process. The AFM indentation was performed on both cleaned and non-cleaned surface. Additional nanoindentation was performed only on a cleaned surface. It turns out the AFM results on the cleaned surface are almost equal to the results from nanoindentation, whereas the AFM results on non-cleaned surface are much smaller. It proves the existence of a softened damaged layer as expected. It also shows that any remaining damaged layer after the cleaning process does not affect the AFM results.

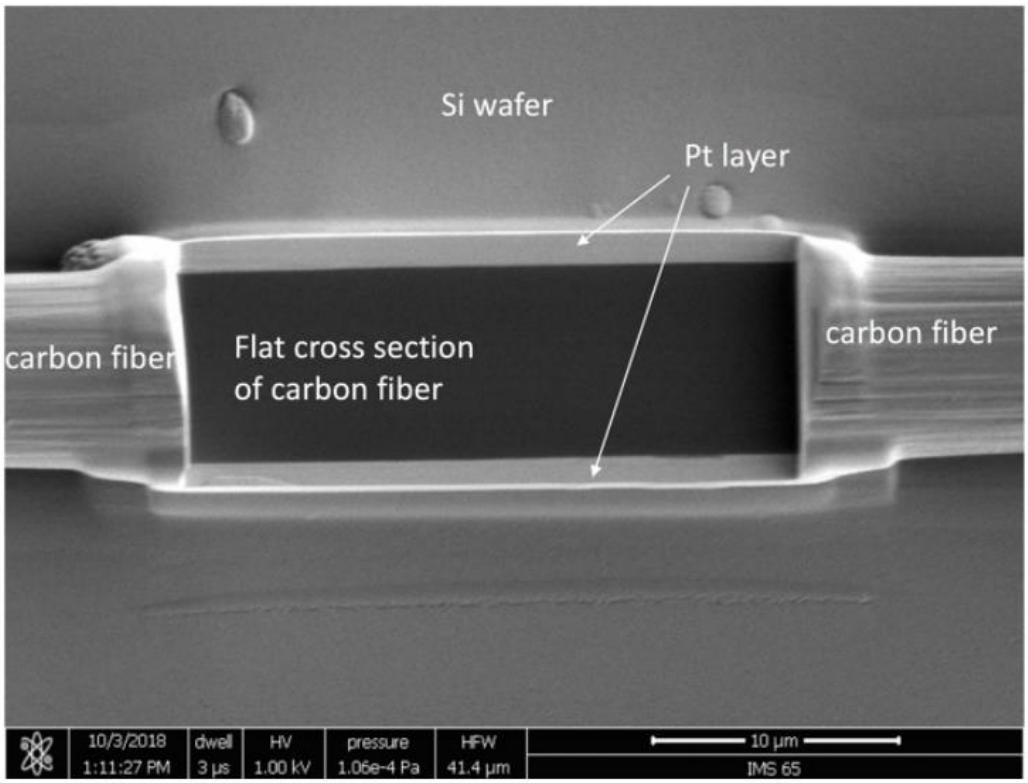

Figure 5. SEM picture of the FIB milled carbon fibre (**Paper A**).

4 Hysteresis behaviour of carbon fibre

Carbon fibres are almost always treated as having constant elastic modulus. However, we found a big difference in indentation modulus when different instruments were used. When the indentation was applied in the fibre axial direction, a deeper nanoindentation test showed a much lower indentation modulus than a shallow AFM indentation (**Paper C**). The indentation modulus in both cases were calculated from the pure elastic region. For the AFM test, the data sets are from the initial loading curve. For nanoindentation test, the data sets are from the initial unloading curve. There is very low risk that plastic deformation in AFM test, since we chose the data region where a constant indentation modulus is obtained. If plastic deformation would occur in the AFM test, the results would be lower instead of higher. The much higher AFM indentation modulus measured is therefore not from an experimental error.

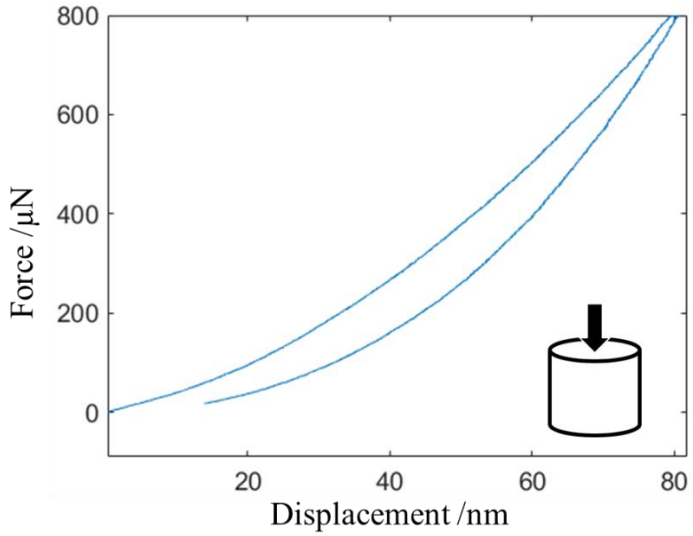

Figure 6. A nanoindentation curve of IMS65 on transverse fibre cross-section (**Paper C**).

A more obvious evidence of the hysteresis behaviour is the nanoindentation curve that showed a fully revisable but not identical loading and unloading curve (Fig. 6). Interestingly, there are numbers of papers in the literature that show nanoindentation curves with same feature [16-20]. However, none of these discussed the reason behind it. In **paper C**, we proposed two plausible explanations. One is based on reversible plastic response [21] and another one is based on nano-buckling of graphene layers in carbon fibre.

Both explanations indicate the lower modulus measured in nanoindentation tests may result from other mechanisms rather than pure elastic deformation. Therefore, the results obtained from AFM were selected as input in the following analysis model.

5 Swanson's model for Hertzian contact of orthotropic materials

The indentation involves compression deformation in all directions and shear deformation. In an isotropic material, both independent elastic constants Young's modulus E and Poisson's ratio υ influence the indentation modulus E^*as

$$E^* = f(E, \upsilon) = \frac{E}{1 - \upsilon^2} \tag{13}$$

However, carbon fibre is a transversely isotropic material. As shown in Fig. 7, there are five independent elastic constants: Young's modulus in fibre direction E_L and in transverse direction E_T, major Poisson's ratio ν_{LT}, transverse Poisson's ratio ν_{TT} and the shear modulus G_{LT}. Therefore, the indentation modulus should be a function of all five elastic constants,

$$E^* = f(E_L, E_T, \nu_{LT}, \nu_{TT}, G_{LT}) \tag{14}$$

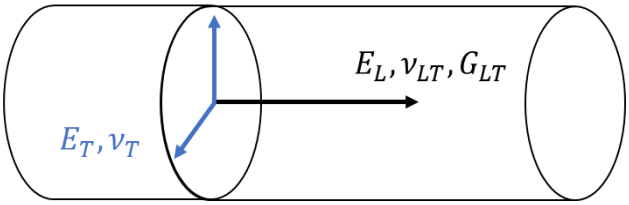

Figure 7. The five independent elastic constants of a carbon fibre.

To analyse the indentation moduli from an indentation experiment, Swanson's orthotropic model was applied [10]. He started from a point load on an orthotropic plane and integrated the surface load to calculate the indentation depth. Unfortunately, there are no analytical expressions. Elastic constants need to be predefined for the calculation. Since the material is orthotropic, the contact area is an ellipse instead of a circular shape. The calculation also must start with an assumption of a circular contact area and then be back-calculated to achieve the ratio of the long and short axis of the elliptical contact area. The new ratio is then applied in a new calculation iteration and a new back-calculated ratio is compared with the previous. The iteration is continued until the calculated value converges, i.e. the difference between the predicted and back-calculated values is small (0.0001 is used here). The calculation workflow is shown in Fig. 8.

Although, Swanson's model allows one to combine all elastic constants to calculate the corresponding indentation modulus, one cannot directly obtain all elastic constants from one indentation modulus. To extract the transverse and shear moduli from the indentation tests, we used the value of the longitudinal Young's modulus E_L provided by the manufacturer and assumed values for Poisson's ratios ν_{LT}, ν_{TT}. We further performed indentation tests on two different surfaces. The impact from assumed

Poisson's ratios was also studied and proven to be very small (**Paper C**). As a consequence, the Eq. 14 was reduced to,

$$E^* = f(E_T, G_{LT}) \tag{15}$$

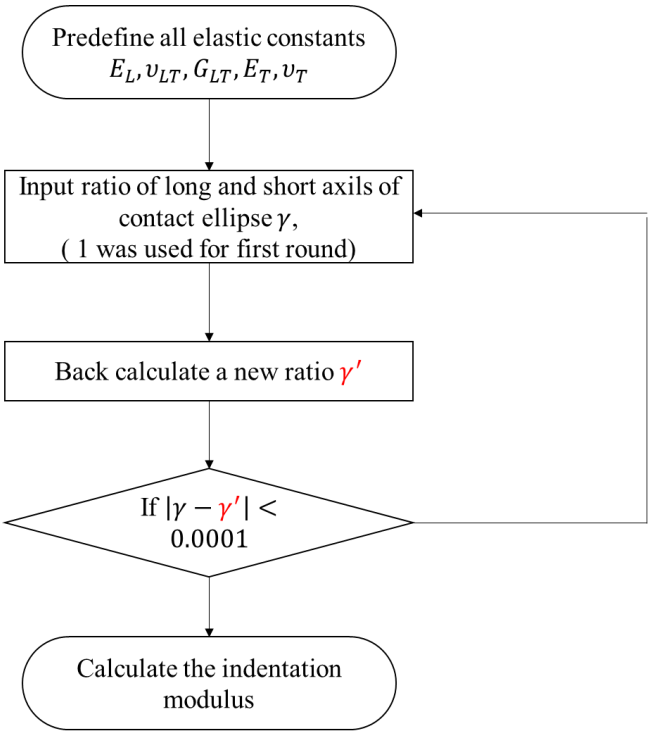

Figure 8. Workflow of Swanson's model.

Predefining E_T and G_{LT}, a contour map of E^* can be calculated as shown in Fig. 9. The experimental results E^* from indentations on the longitudinal and transverse cross-sections determines one curve in this contour map, respectively. The two sought values, E_T and G_{LT}, are determined at their intersection point. In **Paper C**, we successfully determined both E_T and G_{LT} for three different carbon fibres.

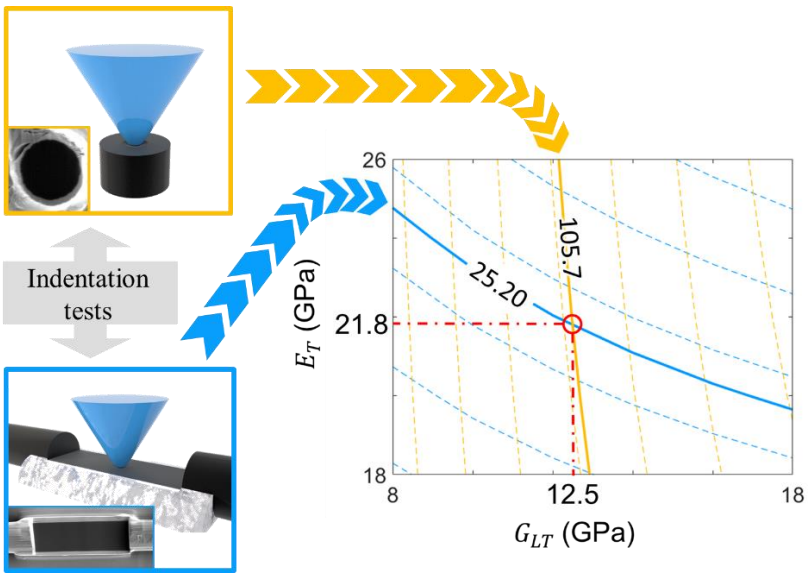

Figure 9. Schematic diagram of the analysis method.

6 Summaries of appended papers

Paper A: Specimen preparation for transverse modulus measurement of carbon fibres using focused ion beam

In this work, we developed an experimental procedure for fabrication of extremely flat surfaces on carbon fibres using FIB. In a FIB milling process, high energy Ga^+ ions were shot on the carbon fibre and knocked out the carbon atoms. The FIB milling is proven to be a very effective tool to mill carbon fibre and both the milling position and angle can be precisely controlled.

Paper B: Transverse modulus measurement of carbon fibre by Atomic Force Microscope and nanoindentation

Surface damage is unavoidable during FIB milling. Such damage would influence the indentation results and therefore a cleaning process is needed. In this work, we performed conventional cleaning method of using low energy Ga^+ ions at low incident angle. The effect from cleaning is studied by comparing indentation results using nanoindentation and AFM. The results show that a soft damage layer forms during the FIB-milling process. The results further imply that influence of any remaining damage layer on the indentation modulus can be neglected after cleaning.

Paper C: Determination of transverse and shear moduli of single carbon fibres

In this paper, we fabricated flat surfaces on carbon fibres using the experiment method developed in **Papers A** and **B**. Both cross-sections in longitudinal (parallel with fibre) and transverse (perpendicular to fibre) directions were fabricated. Indentation tests were performed on these cross-sections using both nanoindentation and AFM. Hysteresis behaviour of carbon fibres was observed when nanoindentation tests were performed on the transverse fibre cross-sections. Indentation moduli E^* were obtained in two directions. Contour maps of E^* on transverse Young's modulus E_T and shear modulus G_{LT} were calculated using Swanson's orthotropic model. The experimental results E^* were then fitted into the contour maps and both transverse and shear moduli were successfully determined.

7 Conclusion and future work

Carbon fibres are highly attractive in lightweight structures due to their outstanding mechanical properties. However, data for the transverse and shear moduli of carbon fibres is still lacking due to the micro-scale dimension of the carbon fibre diameter and its highly anisotropic elastic properties. Furthermore, this lack of data mirrors the lack of a reliable method to measure the full set of elastic properties of single carbon fibres.

In this thesis, we developed an experimental and an analysis method to determine both transverse and shear modulus of carbon fibres. In **Paper A**, we successfully fabricated flat surfaces on carbon fibres with defined position and angle using FIB. The FIB milling process is well-known to destroying the crystal structure at the machined surface. This is of concern since the subsequent indentation test is performed on that surface. To obtain the accurate indentation modulus of the carbon fibre crystal structure, the FIB damaged surface needs to be eliminated as much as possible. In **Paper B**, we polished the surface using low energy ions. By comparing the indentation results on cleaned and non-cleaned surface, it was concluded that the cleaning process eliminates any impact from the damaged layer on indentation modulus. In **Paper C**, flat surfaces on carbon fibre in both fibre and transverse directions were fabricated. Indentation tests were performed in two different directions. A hysteresis indentation behaviour was observed. Employing an orthotropic contact model, the indentation moduli in two directions the transverse and shear moduli were successfully determined.

The developed method in this thesis will be used to study the mechanical properties of lithiated carbon fibres. A lithiated carbon fibre is a carbon fibre with lithium atoms inserted between its graphene layers. The transverse Young's modulus is expected to increase after lithium intersection because the lithium ions strengthen the bonds between graphene layers (from a week van der Waals bond to a strong covalent bond) [21]. The change of mechanical properties is especially important for a structural battery, where carbon fibres serve as anode electrode in a lithium ion battery and become lithiated during battery cycling [22]. The structural battery is in a solid state. A change in mechanical properties, in combination with volume change associated with the state of charge, may introduce internal cracks and failure of the battery. Accurate knowledge of the mechanical properties of lithiated carbon fibre are essential for a reliable design and analysis of the structural battery composite.

Reference

[1] Liu Y, Zwingmann B, Schlaich M, Carbon Fiber Reinforced Polymer for Cable Structures—A Review, Polymers 2015, 7(10): 2078-99.

[2] Asp LE, Berglund LA, Talreja R, Prediction of matrix-initiated transverse failure in polymer composites, Composites Science and Technology 1996; 56 (9):1089-97.

[3] Herráez M, Mora D, Naya F, Lopez CS, González C, Llorca J. Transverse cracking of cross-ply laminates: A computational micromechanics perspective, Composites Science and Technology 2015; 110:195-204.

[4] Maurin R, Davies P, Baral N, Baley C. Transverse properties of carbon fibres by nano-indentation and micro-mechanics. Applied Composite Materials 2008; 15(2):61-73.

[5] Miyagawa H, Mase T, Sato C, Drown E, Drzal LT, Ikegami K. Comparison of experimental and theoretical transverse elastic modulus of carbon fibers. Carbon 2006; 44(10):2008-08.

[6] Mounier D, Poilâne V, Bûcher C, Picart P. Evaluation of transverse elastic properties of fibers used in composite materials by laser resonant ultrasound spectroscopy. Société Française d'Acoustique. Acoustics 2012.

[7] Fujita K, Sawada Y, Nakanishi Y. Effect of cross-sectional textures on transverse compressive properties of Pitch-based carbon fibers. Materials science research international 2001; 7(2):116-21.

[8] Naito K, Tanaka Y, Yang JM. Transverse compressive properties of polyacrylonitrile (PAN)-based and pitch-based single carbon fibers. Carbon 2017; 118:168-83.

[9] Csanádi T, Németh D, Zhang C, Duszaac J. Nanoindentation derived elastic constants of carbon fibres and their nanostructural based predictions. Carbon 2017; 119:314-25.

[10] Swanson SR. Hertzian contact of orthotropic materials. International Journal of Solids and Structures 2004; 41(7):1945-1959.

[11] Oliver WC, Pharr GM. An improved technique for determining hardness and elastic modulus using load and displacement sensing indentation experiments. Journal of Materials Research 1992; 7(6):1564-83.

[12] Hertz H, Über die Berührung fester elastischer Körper, Journal für die reine und angewandte Mathematik 1881; 92:156-71. Germany.

[13] Mayer J, Giannuzzi LA, Kamino T, Michael J. TEM sample preparation and FIB-induced damage. MRS Bulletin 2007; 32(5):400-7.

[14] Rubanov S, Munroe P, Prawer S, Jamieson DN. Surface damage in silicon after 30 KeV Ga FIB fabrication. Microscopy and Microanalysis 2009; 9(S02):884-5.

[15] Giannuzzi LA, Geurts R, Ringnalda J. 2 keV Ga+ FIB milling for reducing amorphous damage in silicon. Microscopy and Microanalysis 2005; 11(S02):828-9.

[16] Ozcan S, Tezcan J, Filip P. Microstructure and elastic properties of individual components of C/C composites. Carbon 2009; 47 (15): 3403-14.
[17] Diss P, Lamon J, Carpentier L, Loubet JL, Kapsa PH, Sharp indentation behavior of carbon/carbon composites and varieties of carbon, Carbon 2002; 40 (14): 2567-79.
[18] Marx DT, Riester L, Mechanical properties of carbon—carbon composite components determined using nanoindentation, Carbon 1999; 37(11): 1679-84. https://doi.org/10.1016/S0008-6223(98)00239-5
[19] Kanari M, Tanaka K, Baba S, Eto M, Nanoindentation behavior of a two-dimensional carbon-carbon composite for nuclear applications, Carbon 1997; 35(10-11): 1429-37
[20] Leatherbarrow A, Wu H, Mechanical behaviour of the constituents inside carbon-fibre/carbon-silicon carbide composites characterised by nano-indentation, J. Euro. Ceram. Soc. 2012; 32(3): 579-588.
[21] Kganyago KR and Ngoepe PE, Ab initio calculation of the voltage profile for LiC_6, Solid State Ionics 2003; 159(1-2):21-23.
[22] Asp LE and Greenhalgh ES, Structural power composites. Composites Sciences and Technology 2014; 101:41-46.